

# Assessing the global conservation status of the rock rose *Helianthemum caput-felis*

ELENA SULIS, GIANLUIGI BACCHETTA, DONATELLA COGONI, DOMENICO GARGANO and GIUSEPPE FENU

SUPPLEMENTARY TABLE 1 List of online databases and herbaria consulted.

	Source/Location
<b>Online databases</b>	
Global Biodiversity Information Facility	<a href="http://www.gbif.org/occurrence">http://www.gbif.org/occurrence</a>
African Plant Database	<a href="http://www.ville-ge.ch/musinfo/bd/cjb/africa">http://www.ville-ge.ch/musinfo/bd/cjb/africa</a>
Anthos—Sistema de información sobre las plantas de España	<a href="http://www.anthos.es">http://www.anthos.es</a>
Banco de datos de Biodiversidad—Generalitat Valenciana	<a href="http://bdb.cma.gva.es">http://bdb.cma.gva.es</a>
Ministero dell'Ambiente e della Tutela del Territorio e del Mare (MATTM) & Istituto superiore per la protezione e la ricerca ambientale-(ISPRA)	<a href="http://www.reportingdirettivahabitat.it">http://www.reportingdirettivahabitat.it</a>
<b>Herbaria*</b>	
AL	University of Algiers (Algeria)
BC	Botanical Institute of Barcelona (Spain)
CAG	University of Cagliari (Italy)
GDA	University of Granada
HJBS	The Sóller Botanic Garden Herbarium (Spain)
MA	Real Jardín Botánico of Madrid (Spain)
MGC	University of Malaga (Spain)
MPU	University of Montpellier (France)
P	Muséum National d'Histoire Naturelle–Paris (France)
SASSA	Faculty of Sciences, University of Sassari (Italy)
SEV	University of Sevilla (Spain)
SS	Faculty of Pharmacy, University of Sassari (Italy)
VAL	University of Valencia (Spain)

\*Abbreviations follow Thiers (2018).

SUPPLEMENTARY MATERIAL 1 Estimating *Helianthemum caput-felis* extinction risk using the E criterion of the IUCN Red List criteria: methodological details and implementation of models.

## Data collection

Demographic data were collected on 98 permanent plots placed in six different populations along the overall species distribution range and representative of the full ecological range in which the plant grows (Sulis et al., 2018). In each population, after excluding the areas with extreme conditions, permanent plots (2 × 1 m in size) were randomly placed in the area where the plant was found; within the plots, all present plants (821 in the first census) were marked, mapped and monitored over a three-year period (2013–2015; Sulis et al., 2018). All new seedlings that appeared inside the plots were also counted, measured and mapped. Surveys took place three times per year, following Jacquemyn et al. (2010). In early March, all plots were surveyed for the first time to locate all previously mapped individual plants and to map any new seedlings. During the flowering peak (March–April), when all the plants were fully grown, the plots were surveyed a second time to measure each plant (i.e. height, minimum and maximum diameter), to count the number of flowers per plant and to check for the occasional new individuals, which were added to the data set. During the fruiting peak (late May–early June), the last survey was made on all plots to estimate the number of fruits per plant. In this case, 10 mature fruits were randomly collected from each plot to estimate the mean number of seeds per fruit (N = 980 fruits in total). The number of seeds per fruit was directly counted in the laboratory, and subsequently, the number of seeds for each plant was estimated by multiplying the average number of seeds per fruit and the number of fruits per plant (Sulis et al., 2018). All the collected data were organized in a global geo-database.

## Description and implementation of models

Population models provide a powerful tool for population biologists to estimate parameters important to population persistence and dynamics by modelling commonly collected demographic data on stage and/or age transitions (Caswell, 2001). These models may result in biases, however, where underlying state variables are continuous (Picard et al., 2010; Salguero-Gómez & Plotkin, 2010), such as for example, height, weight, biomass (Metcalf et al., 2013). These models quantify all ways (through survival and reproduction) in which individuals contribute to the size of the population after one-time step. Transition matrices contain exactly the same information as life cycle graphs, but then organized in matrix form. Hence, matrix models represent the life cycle of individuals, and can be used to investigate the dynamics of a population (Jongejans & de Kroon, 2012). A transition matrix (A) consists of matrix elements ( $a_{ij}$ ) which describe survival, growth and fecundity transitions from stage  $j$  to stage  $i$  during a certain period of time. Perturbation analyses of the demographic matrices, such as elasticity analysis, are used to determine which hypothetical changes in matrix elements ( $a_{ij}$ ) have the greatest effects on the deterministic population growth rate ( $\lambda$ ). The deterministic population growth rate denotes the asymptotic growth of the population, which can indicate an increasing, stable or declining population (Ramula, 2008).

Recently, a new discrete-time structured method has been introduced: the integral projection model (Easterling et al., 2000), which retains the desirable properties of the matrix projection model while avoiding entirely the need to group plants into discrete stage classes. Integral projection models describe how a population structured by a continuous individual-level state variable changes in discrete time (Easterling et al., 2000). Integral projection models are defined by a kernel, which represents probability densities of growth between discrete or continuous stages conditional on survival, and the production of offspring (Metcalf et al., 2013). It offers tools that can incorporate stage, age and continuous states into similar analysis of population dynamics (Easterling et al., 2000; Ellner & Rees, 2006).

The main difference between an integral projection model and a matrix population model is that whereas in discrete projection matrices the number of classes (i.e. number of stages in the life cycle of the study species) must be defined a priori, integral projection models impose the discretization of the three-dimensional surface for the purposes of numerical integration. This produces a typically large matrix (e.g.  $100 \times 100$  cells) that is more robust to biases from matrix dimensionality (Zuidema et al., 2010; Salguero-Gómez & Plotkin, 2010) and sample size (e.g. Ramula et al., 2009) than classical matrix models (Metcalf et al., 2014).

To investigate the demography of the *H. caput-felis* global population both the matrix population model and the integral projection model were performed. In a constant environment, a modelled asymptotic growth rate ( $\lambda$ )  $> 1$  indicates that the population will eventually increase whereas  $\lambda < 1$  indicates that the population will decline to extinction (Ezard et al., 2010).

The chosen variable (to define the size-classes in the matrix population model and as continuous state variable in the integral projection model ) to evaluate the demographic dynamics of *H. caput-felis* populations was plant size (plant volume) which has been demonstrated to be positive correlated with the reproductive capacity (Fenu et al., 2015). The plant volume (plant size =  $V$ , expressed in  $\text{cm}^3$ ) was calculated according to the formula in Fenu et al. (2015):

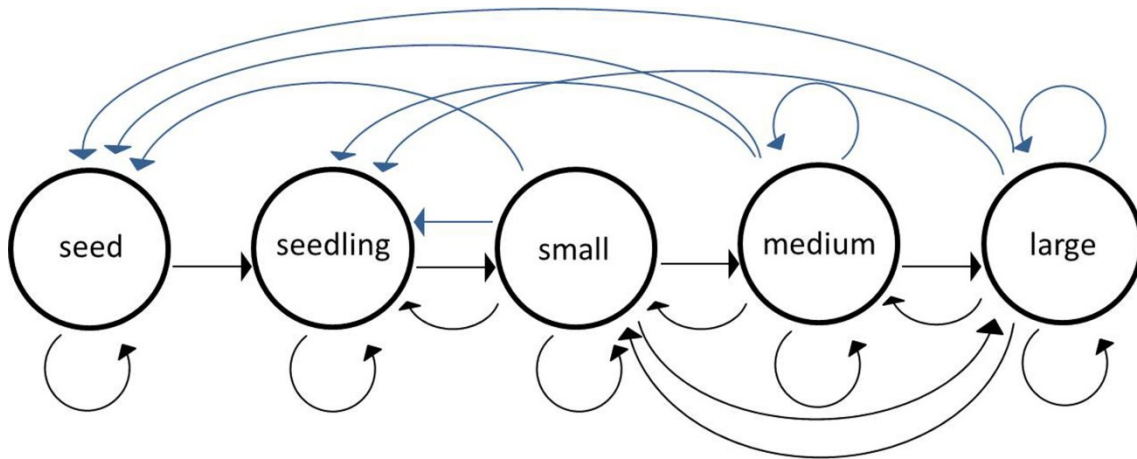
$$\text{Plant size [cm}^3\text{]: } V = [\pi \times (d_M/2) \times (d_m/2)] \times h$$

in which plant height ( $h$ ) and the maximum and minimum diameter ( $d_M$  and  $d_m$ , respectively) directly measured for each individual plant were used.

#### *Matrix population model implementation*

To characterize the population dynamics of *H. caput-felis*, a size-structured matrix model was constructed (Caswell, 2001), from which demographic vital rates and their relative importance were calculated. Matrix models divide the populations into discrete classes and track the contribution of individuals in each class at one census to all classes in the following census (Caswell, 2001; Morris & Doak, 2002). This stage classification was devised to characterize the population using a biological approach (Lefkovitch, 1965; Marrero-Gómez et al., 2007), which relies on field observations of developmental states. The life cycle of *H. caput-felis* was classified into five developmental stages based on the results of a previous study (Fenu et al., 2015) and on our field observations. Accordingly, a seed bank class, a seedling class and three adult classes (small, medium and large) were distinguished, based on plant size (plant volume) and the reproductive capacity (number of fruits per plant). Hence, five size classes were selected to build the matrices: (1) seeds, (2) plants with a volume  $< 5 \text{ cm}^3$  (seedling, hereafter), (3) flowering and fruiting plants with a volume of  $5.1\text{--}500 \text{ cm}^3$  (small adult, hereafter), (4) adults plants with a volume of  $500.1\text{--}5000 \text{ cm}^3$  (medium adult, hereafter), and (5) large adults plants (large, hereafter).

The seed bank class was calculated by multiplying the proportion of total reproductive output attributable to an individual (the average number of seeds per fruit with the fruit number of each plant; data from Fenu et al., 2015) times the total number of seedlings at the end of the projection interval (Stubben & Milligan, 2007). According to Wardle (1998), the transitions among the different life stages are shown in the life-cycle diagram in Supplementary Fig. 1.



SUPPLEMENTARY FIG. 1 Life cycle diagram of *Helianthemum caput-felis*. The black arrows represent survival/growth transitions and the blue arrows involve production (via seeds) of new individuals after one year.

The basic matrix model is given by

$$n_{t+1} = A n_t$$

where  $n_t$  and  $n_{(t+1)}$  are vectors whose elements,  $a_{ij}$  are the number of individuals that belong to the  $i$ th category at time  $t$  and  $t + 1$ , respectively, and  $A$  is the non-negative square matrix, whose elements,  $a_{ij}$  represent the transitions or contributions from individuals in the  $j$ th category to the  $i$ th category after one-time step (Caswell, 2001). Transition probabilities were obtained by calculating the proportion of individuals in each category experiencing each specific fate from one year to the next (Marrero-Gómez et al., 2007).

The survival rate is the expected proportions of plants in class  $i$  at the last census that are still alive at the current census. The growth rate is the estimated probability that a surviving plant undergoes a transition from its original class to each of the other potential classes (Morris & Doak, 2002).

A different transition matrix for each year was generated, adding individual fertility estimates per plant. Then, the annual matrices were created setting the number of time steps for a deterministic model ( $it=100$ ). To extract the mean deterministic  $\lambda$  of all years, a mean of the three projection matrices for deterministic analysis was calculated, making random draw with replacement.

Long-term simulations of the fates of *H. caput-felis* population were carried out by incorporating environmental stochasticity into the matrix models. Environmental stochasticity involves chance variation in several external factors such as weather conditions that affect population performance (Picó & Riba, 2002). The effect of initial population size on the long-term dynamics of the analysed population was tested in order to calculate the stochastic growth rate ( $\lambda_s$ , Tuljapurkar et al., 2003). The numeric values for the population size (40 seedlings, 186 small, 210 adults and 209 large adults plants) in the first year of monitoring (2013) were used as starting population vector ( $n_t$ ).

The *popbio* 2.4.3 package of Stubben & Milligan (2007) in *R* 3.1.2 (R Core Team, 2014) was used to calculate the finite rate of increase ( $\lambda$ ) and the stochastic lambda ( $\lambda_s$ ) of the population via Tuljapakar's method (Tuljapurkar, 1990). The bootstrap method (Kalisz & McPeck, 1993; Caswell, 2001) was used: each annual matrix was randomly resampled with replacement 50,000 times. Therefore, in each sample, the number of plants in each size class equalled the number in the corresponding class in the original data set; then, from the resulting distributions of 50,000 estimates for each matrix, the stochastic growth rate was extracted (the analytic approximation of  $\lambda$

and a percentile 95% confidence interval were computed; Morris & Doak, 2005). Bootstrap distributions of population growth rates were calculated using the *boot.transitions* function of the aforementioned package.

### Integral projection model implementation

Integral projection models are similar to matrix population models, but differ because populations do not have to be divided into classes, but state variables (size, in this case) can be continuous (Easterling et al., 2000). Integral projection models describe how a population structured by a continuous individual-level state variable changes in discrete time (Easterling et al., 2000), using a continuous projection kernel to describe the population size distribution by a density function (Easterling et al., 2000; Ellner & Rees, 2006). The state of the population is described by the size distribution  $n(y, t)$ , and growth, survival, flowering and fruiting probability are described in function of the selected continuous variable (plant size = plant volume). Constant, linear and quadratic models were fitted for each vital rate, and the best model was selected based on the lowest AIC value (Dauer & Jongejans, 2013). The integral projection model of a size structured population is given by:

$$n(y, t+1) = \int_L^U K(y, x) n(x, t) dx = \int_L^U [P(y, x) + F(y, x)] n(x, t) dx$$

where  $n(y, t + 1)$  is the size distribution  $y$  of both established and newly recruited plants in census time  $t + 1$ ,  $n(x, t)$  the distribution across size of individuals at census time  $t$ ,  $L$  and  $U$  are the respective lower and upper size limits modelled in the integral projection model (Metcalf et al., 2013), and these values were set lower and higher than the observed minimum and maximum sizes, to avoid unintentional evictions (Williams et al., 2012).

The kernel ( $K$ ) can be broken down into two sub-kernels ( $P$  and  $F$ ):  $P$  sub-kernel represents transitions attributable to survival and growth, while  $F$  sub-kernel describes *per capita* contributions of reproductive individuals given the recruit density function at the next census (Metcalf et al., 2013).

Survival, growth and fecundity objects that compose the integral projection model were constructed using the *IPMpack 2.1* package (Metcalf et al., 2014), and matrix were plots with the *fields* package (Nychka et al., 2014) in *R* (R Core Team, 2014).

The method proposed by Merow et al. (2014) for species with complex life cycles was followed and adapted to the specific case of this study. The survival probability was modelled by logistic regression (binomial error distribution and logit link function), and the growth probability was modelled as a linear regression (Merow et al., 2014). Fecundity was the product of two vital rates: the probability of flowering, modelled as a logistic regression (by specifying binomial error distributions and logit-link functions in GLM), and the number of fruits in the peak of the year  $t$  for every monitored plant, modelled as a linear regression (with a Poisson error distribution and a log link function), times the mean number of seedlings in year  $t + 1$  per number of fruiting individuals in year  $t$ , and a probability function of the seedling size distributions. The seedling size distribution in each year was described as a normal distribution with the observed mean and standard deviation (Merow et al., 2014).

Direct determination of further vital rates in the field was impossible for every individual plant, so they were included in the integral projection model as constants (i.e. size independent), and have been incorporated into the fecundity parameter calculation:

- (1) the mean number of seeds per fruit (obtained multiplying the total number of filled fruits directly counted in the field by the mean value of seeds per fruit, following the same approach in Bruna et al. (2014);
- (2) the probability of seed germination, by counting the number of all new seedlings in  $t+1$  compared to the total number of seeds in  $t$ ;
- (3) the probability of seedling survival within the year of seed and seedling production, estimated from the ratio between seedlings counted in year  $t$  and seedlings present in  $t+1$  (Merow et al., 2014);
- (4) the probabilities of seeds entering the seed bank or
- (5) the probability of the seeds staying in that location, calculated according to Quintana-Ascencio et al. (1998) because of the absence of available seed bank studies for *H. caput-felis*.

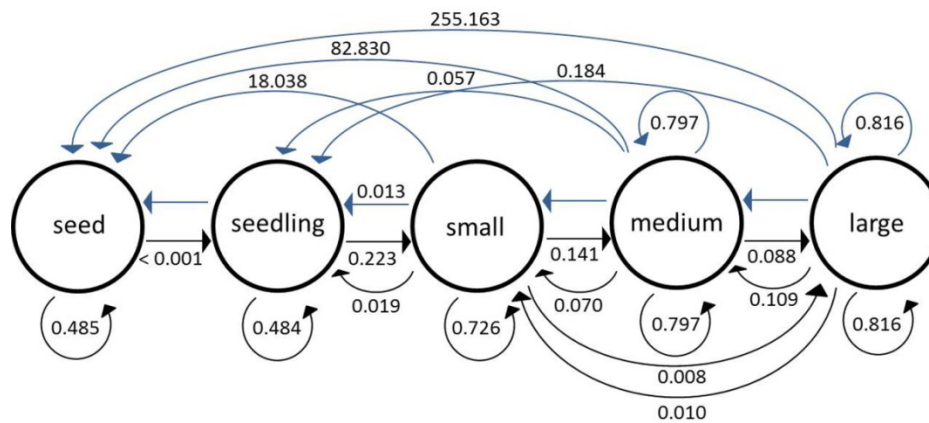
The integral projection model predicts the population's asymptotic growth rate ( $\lambda$ ), represented by the dominant eigenvalue, with associated eigenvectors and state-dependent sensitivity and elasticity functions (Easterling et al., 2000). The dominant right and left eigenvectors  $w(x)$  and  $v(x)$  give the stable size distribution and the size-specific reproductive value, respectively (Easterling et al., 2000). The projected stable size distribution, which is the abundance of plants whose vital rates do not change with time (Caswell, 2001), was extracted and compared with the observed distributions.

Stochastic population growth rates ( $\lambda_s$ ) were calculated by randomly selecting one of three annual matrices with equal probability for each of 1000 model iterations, and taking the geometric mean of the obtained annual growth rates (Caswell, 2001; Morris & Doak, 2002). Then, to estimate sampling errors in  $\lambda_s$ , resampled the data, a bootstrap vector of the same sample size was generated, and  $\lambda$  and bias-corrected 95% confidence intervals (CI) were calculated (Schleuning & Matthies, 2009). Stochastic lambdas provide a more conservative risk assessment than those estimated from mean matrices for species in fluctuating environments (Menges, 2000).

The main outputs of matrix population models and integral projection models are summarized in Table 1. Deterministic population growth rate ( $\lambda$ ) extracted from matrix population models was higher in the first transition year (1.03) compared to the second (0.92). Growth rates calculated considering only the continuous stage (excluding the discrete seed bank stage;  $\lambda_{\text{continuous}}$ ) were slightly lesser from those including the seed bank ( $\lambda$ ). Stochastic growth rate ( $\lambda_s$ ) did not differ from the deterministic rate of the mean matrix ( $\lambda_M$ ). The two projected matrices show how large adult plants gave the major contribution to fecundity, while the proportion of plants along the diagonal is greater than others. The mean projected transition matrix is displayed in Supplementary Fig. 2, represented as a life cycle diagram, which represent the mean transitions between the five different life stages observed in the study population.

SUPPLEMENTARY TABLE 1 Parameters extracted from matrix population models and integral projection models of *H. caput-felis* for the 2-year transitions: projected deterministic population growth rate excluding the seed bank ( $\lambda_{\text{continuous}}$ ), projected deterministic population growth rate ( $\lambda$ ) with confidence intervals at 95%, damping ratio ( $d_r$ ), deterministic population growth rate of the mean projected matrix ( $\lambda_M$ ), and stochastic population growth rate ( $\lambda_S$ ).

	Matrix population model		Integral projection model	
	2013–2014	2014–2015	2013–2014	2014–2015
$\lambda_{\text{continuous}}$	1.01	0.81	1.02	0.92
$\lambda$ [CI]	1.03 [1.002 - 1.054]	0.92 [0.891 - 0.951]	1.08 [1.067 - 1.107]	0.92 [0.918 - 0.926]
$d_r$	1.39	1.38	1.35	1.30
$\lambda_M$	0.98		1.01	
$\lambda_S$	0.97 [0.9729 - 0.9755]		1.00 [-]	



SUPPLEMENTARY FIG. 2 Loop analysis of the life cycle of *H. caput-felis*. Values correspond to P and F values of the mean projected matrix. The black arrows represent survival/growth and the accompanying rates give the proportion of individuals that survive and move to a particular class. The blue arrows involve production (via seeds) of new individuals after 1 year. The projected  $\lambda$  of the mean matrix is 0.98, projecting a decrease in population size of 2% per year.

### Extinction risk estimation

To calculate the quasi-extinction risk for the population of *H. caput-felis* the size-structured matrix model was used. Although integral projection models better perform data of species with restricted range and small demographic data sets ( $< 300$  individuals; Ramula et al., 2009; Sulis, 2016), the R package *IPMpack* does not permit calculation of the quasi-extinction risk probability; for this reason, matrix projection models (matrix population models) were run using the package *popbio* (Stubben & Milligan, 2007).

As a first step, two additional population traits requested for the quasi-extinction risk calculation, were extracted both by the matrix population model and the integral projection model: the net reproductive rate ( $R_0$ ) and the generation time ( $T$ ). The  $R_0$  represents the average number of offspring produced by an individual over its lifespan (Metcalf et al., 2014), and it represents the global population growth rate per generation (not per unit of time), in which population growth is positive if, and only if,  $R_0 > 1$  (Caswell, 2011). The generation time ( $T$ ), considered as the time

required by the population to increase by a factor of  $R_0$  (Caswell, 2001; Williams et al., 2011) and representing also a measure of the typical age at which offspring are produced, was calculated according to the formula:

$$n_{t+1} = A n_t$$

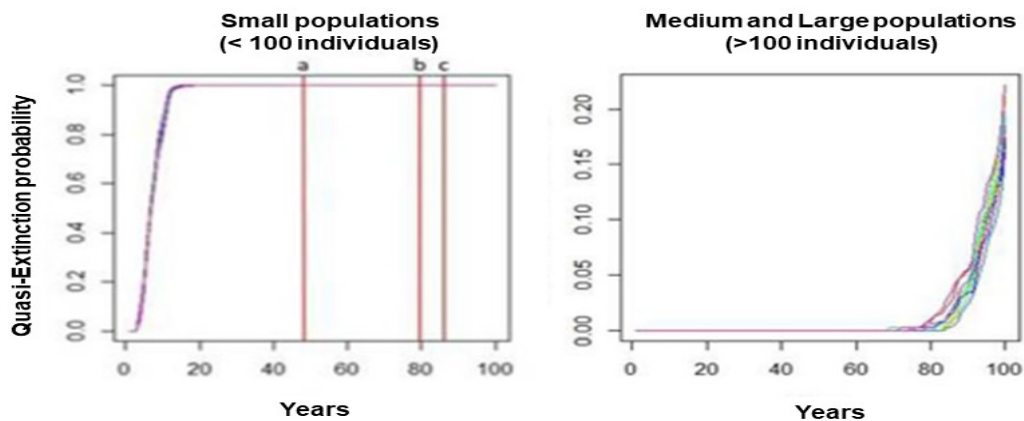
The mean generation time (T) values were calculated both with the integral projection model and matrix population model, to carry out an accurate extinction risk analysis. The net reproductive rate ( $R_0$ ) was  $>1$  in 2013–2014 and  $<1$  in 2014–2015, in both models. The mean generation time (T) from the matrix population model was 28.44 years, whereas from the integral projection model was 15.97 years.

Extinction Probability ( $Pe$ ) was calculated for  $t = 100$  years as the proportion of 500 model iterations where the quasi-extinction threshold was reached (Van der Meer et al., 2014). We calculated mean value of this parameter over 95% confidence intervals by taking the 2.5th and the 97.5th percentile of the simulated distribution (e.g. Shryock et al., 2014; Belaid et al., 2018). Matrices were selected at random with replacement (each matrix had an equal probability of selection; Morris & Doak, 2002). The number of monitored plants in 2013 (i.e. the global population in this study) was used as the population vector (sensu Morris & Doak, 2002) and consisted of 40 seedlings, 186 juveniles, 210 small adults and 209 large adults. A quasi-extinction threshold of 20 mature individuals was designated a priori, to help minimize demographic stochasticity associated with small population size (Morris & Doak, 2002).

The estimation of quasi-extinction risk was calculated using the *popbio* package (Stubben & Milligan, 2007), based upon methods described in Caswell (2001) and Morris & Doak (2002), in R (R Core Team, 2014).

The probability of reaching a quasi-extinction threshold (20 individuals) based on 500 iterations of population growth over 100 years highlighted that small populations will be extinct in a period ranging from 10 to 16 years and, more generally, all populations with  $<100$  individuals achieve the 100% quasi-risk extinction probability before 100 years (67 years on average; Supplementary Fig. 3). Only populations with  $>100$  mature plants face no high risk of extinction according to this models because they will not reach populations sizes of 20 (or fewer) individuals in the next 100 years.





SUPPLEMENTARY FIG. 3 Simulated cumulative distribution functions for the time to reach a quasi-extinction threshold of 20 individuals for small populations (< 100 individuals; **a**: three generations; **b**: five generations; **c**: three generations based on generation time calculated with matrix population model) and medium/large populations (>100 individuals).

## References

- Belaid, A.H., Maurice, S., Fréville, H., Carbonell, D. & Imbert, E. (2018) Predicting population viability of the narrow endemic Mediterranean plant *Centaurea corymbosa* under climate change. *Biological Conservation*, 223, 19–33.
- Bruna, E.M., Izzo, T.J., Inouye, B.D. & Vasconcelos, H.L. (2014) Effect of mutualist partner identity on plant demography. *Ecology*, 95, 3237–3243.
- Caswell, H. (2001) *Matrix population models: construction, analysis, and interpretation*. Sinauer, Sunderland, MA.
- Caswell, H. (2011) Beyond  $R_0$ : demographic models for variability of lifetime reproductive output. *PLoS ONE*, 6, e20809.
- Dauer, J.T. & Jongejans, E. (2013) Elucidating the population dynamics of Japanese Knotweed using Integral Projection Models. *PLoS ONE*, 8, e75181.
- Easterling, M.R., Ellner, S.P. & Dixon, P.M. (2000) Size-specific sensitivity: applying a new structured population model. *Ecology*, 81, 694–708.
- Ellner, S.P. & Rees, M. (2006) Integral projection models for species with complex demography. *The American Naturalist*, 167, 410–428.
- Ezard, H.G., Bullock, J.M., Dalglish, H.J., Millon, A., Pelletier, F. & Ozgul, A. (2010) Matrix models for a changeable world: The importance of transient dynamics in population management. *Journal of Applied Ecology*, 47, 515–523.
- Fenu, G., Cogoni, D., Sulis, E. & Bacchetta, G. (2015) Ecological response to human trampling and conservation status of *Helianthemum caput-felis* (Cistaceae) at the eastern periphery of its range. *Botany Letters*, 162, 191–201.
- Jacquemyn, H., Brys, R. & Jongejans, E. (2010) Size-dependent flowering and costs of reproduction affect population dynamics in a tuberous perennial woodland orchid. *Journal of Ecology*, 98, 1204–1215.

- Jongejans, E. & de Kroon, H. (2012) Matrix models. In *Encyclopedia of Theoretical Ecology* (eds. Hastings, A. & Gross L.), pp. 415–423. University of California, Berkeley and Los Angeles, USA.
- Kalish, S. & McPeck, M.A. (1993) Extinction dynamics, population growth and seed banks. *Oecologia*, 95, 314–320.
- Lefkovich, L.P. (1965) The study of population growth in organisms grouped by stages. *Biometrics*, 21, 1–18.
- Marrero-Gómez, M.V., Oostermeijer, J.G.B., Carqué-Álamo, E. & Bañares-Baudet, Á. (2007) Population viability of the narrow endemic *Helianthemum juliae* (Cistaceae) in relation to climate variability. *Biological Conservation*, 136, 552–562.
- Menges, E.S. (2000) Population viability analyses in plants: challenges and opportunities. *Trends in Ecology and Evolution*, 15, 51–56.
- Merow, C., Latimer, A.M., Wilson, A.M., McMahon, S.M., Rebelo, A.G. & Silander, J.A. (2014) On using integral projection models to generate demographically driven predictions of species' distributions: development and validation using sparse data. *Ecography*, 37, 1167–1183.
- Metcalf, C.J.E., McMahon, S.M., Salguero-Gómez, R. & Jongejans, E. (2013) IPMpack: an R package for integral projection models. *Methods in Ecology and Evolution*, 4, 195–200.
- Metcalf, C.J.E., McMahon, S.M., Salguero-Gómez, R., Jongejans, E. & Merow, C. (2014) IPMpack: an R package for demographic modeling with Integral Projection Models (v. 2.1). [accessed 8 May 2017].
- Morris, W.F. & Doak, D.F. (2002) *Quantitative Conservation Biology: The Theory and Practice of Population Viability Analysis*. Sinauer Associates, Sunderland, USA.
- Morris, W.F. & Doak, D.F. (2005) How general are the determinants of the stochastic population growth rate across nearby sites? *Ecological Monographs*, 75, 119–137.
- Nychka, D., Furrer, R. & Sain, S. (2014) fields: Tools for spatial data. R package version 7.1. <http://CRAN.R-project.org/package=fields> [accessed on 8 May 2018].
- Picard, N., Ouédraogo, D. & Bar-Hen, A. (2010) Choosing classes for size projection matrix models. *Ecological Modelling*, 221, 2270–2279.
- Picó, F.X. & Riba, M. (2002) Regional-scale demography of *Ramonda myconi*: Remnant population dynamics in a preglacial relict species. *Plant Ecology*, 161, 1–13.
- Quintana-Ascencio, P.F., Dolan, R.W. & Menges, E.S. 1998. *Hypericum cumulicola* demography in unoccupied and occupied Florida scrub patches with different time-since-fire. *Journal of Ecology*, 86, 640–651.
- R Core Team (2014) *R: A Language and Environment for Statistical Computing*. R Foundation for Statistical Computing, Vienna, Austria. <http://www.R-project.org/> [accessed 8 May 2017].
- Ramula, S. (2008) Responses to the timing of damage in an annual herb: fitness components versus population performance. *Basic and Applied Ecology*, 9, 233–242.
- Ramula, S., Rees, M. & Buckley, Y.M. (2009) Integral projection models perform better for small demographic data sets than matrix population models: a case study of two perennial herbs. *Journal of Applied Ecology*, 46, 1048–1053.
- Salguero-Gómez, R. & Plotkin, J.B. (2010) Matrix dimensions bias demographic inferences: implications for comparative plant demography. *The American Naturalist*, 176, 710–722.
- Schleuning, M. & Matthies, D. (2009) Habitat change and plant demography: assessing the extinction risk of a formerly common grassland perennial. *Conservation Biology*, 23, 174–183.
- Shryock, D.F., Esque, T.C. & Hughes, L. (2014) Population viability of *Pediocactus bradyi* (Cactaceae) in a changing climate. *American Journal of Botany*, 101, 1944–1953.
- Stubben, C. & Milligan, B. (2007) Estimating and analyzing demographic models using the popbio package in R. *Journal of Statistical Software*, 22, 1–23.
- Sulis, E. (2016) *Ecological features, populations traits and conservation status of Helianthemum caput-felis along its distribution range*. PhD. Thesis. University of Cagliari, Cagliari, Italy.

- Sulis, E., Bacchetta, G., Cogoni, D. & Fenu, G. (2018) Short-term population dynamics of *Helianthemum caput-felis*, a perennial Mediterranean coastal plant: a key element for an effective conservation program. *Systematics and Biodiversity*, in press. <https://doi.org.10.1080/14772000.2018.1492469>
- Thiers B. (2018) *Index Herbariorum: A Global Directory of Public Herbaria and Associated Staff*. New York Botanical Garden's Virtual Herbarium. <http://sweetgum.nybg.org/science/ih/>. [accessed 8 September 2018].
- Tuljapurkar, S. (1990) *Population Dynamics in Variable Environments*. Springer-Verlag, New York, USA.
- Tuljapurkar, S., Horvitz, C.C. & Pascarella, J.B. (2003) The many growth rates and elasticities of populations in random environments. *The American Naturalist*, 162, 489–502.
- Van der Meer, S., Dahlgren, J.P., Mildén, M. & Ehrlén, J. (2014) Differential effects of abandonment on the demography of the grassland perennial *Succisa pratensis*. *Population Ecology*, 56, 151–160.
- Wardle, G.M. (1998) A graph theory approach to demographic loop analysis. *Ecology*, 79, 2539–2549.
- Williams, J.L., Ellis, M.M., Bricker, M.C., Brodie, J.F. & Parsons, E.W. (2011) Distance to stable stage distribution in plant populations and implications for near-term population projections. *Journal of Ecology*, 99, 1171–1178.
- Williams, J.L., Miller, T.E. & Ellner, S.P. (2012) Avoiding unintentional eviction from integral projection models. *Ecology*, 93, 2008–2014.
- Zuidema, P.A., Jongejans, E., Chien, P.D., During, H.J. & Schieving, F. (2010) Integral projection models for trees: a new parameterization method and a validation of model output. *Journal of Ecology*, 98, 345–355.